



# On the Expedient Solution of the Boltzmann Equation by Modified Time Relaxed Monte Carlo (MTRMC) Method

M. Eskandari<sup>1</sup> and S. S. Nourazar<sup>1†</sup>

*Department of Mechanical Engineering, Amirkabir University of Technology, Tehran, Iran*

†Corresponding Author Email: [icp@aut.ac.ir](mailto:icp@aut.ac.ir)

(Received May 16, 2017; accepted January 6, 2018)

## ABSTRACT

In the present study, a modified time relaxed Monte Carlo (MTRMC) method is developed for numerical solution of the Boltzmann equation in rarefied regimes. Taylor series expansion is employed to obtain a generalized form of the Wild sum expansion and consequently the modified collision functions with fewer inter-molecular interactions are obtained. The proposed algorithm is applied on the lid-driven micro cavity flow with different lid velocities and the results for velocity and shear stress distributions are compared with those from the standard DSMC and TRMC methods. The comparisons show excellent agreement between the results of the MTRMC method with their counterparts from TRMC and DSMC methods. The present study illustrates appreciable improvement in the computational expense of the MTRMC method compared to those from standard TRMC and DSMC methods. The improvement is more pronounced compared to the standard DSMC method. It is observed that up to 56% reduction in CPU time is obtained in the studied cases.

**Keywords:** Boltzmann equation, Time relaxed Monte Carlo, modified time relaxed Monte Carlo, direct simulation Monte Carlo, Taylor series

## NOMENCLATURE

$F$	transformed probability distribution function	$t$	time
$f$	probability distribution function	$U$	velocity
$Kfn$	Knudsen number	$v$	velocity vector
$L$	the characteristic length scale of the flow	$x,y$	x and y directions, respectively
$lid$	moving lid	$\mu$	the mean collision frequency, kinematic viscosity
$M$	local Maxwellian distribution	$\tau$	relaxed time, shear stress
$P$	collisional operator	$0$	initial condition
$Q$	collisional operator		

## 1. INTRODUCTION

The Navier-Stokes equations lose the accuracy of simulating the flows when the characteristic length of the flow becomes comparable to the mean free path. In this circumstance, the governing equation is the Boltzmann equation of kinetic theory (Cercignani 1988; Bird 1994). During the past decades, direct simulation Monte Carlo (DSMC) method has been extensively adopted for the numerical solution of the Boltzmann equation in rarefied regimes (Cercignani 1988; Bird 1994; Pareschi and Trazzi 2005). Despite the simplicity and reasonable accuracy of the DSMC method, computational expense of the method cannot be justified as the flow nears the continuum region.

Hence, the challenge is to reduce the computational CPU time of numerical solution of the Boltzmann equation (Pareschi and Trazzi 2005; Oran, E.S., Oh, C.K., and Cybyk 1998; Gabetta, Pareschi, and Toscani 1997; Pan, Liu, Khoo, and Song 2000; Filbet and Russo 2003).

Recently, time relaxed Monte Carlo (TRMC) method has been introduced as a simple and efficient numerical method to solve the Boltzmann equation in the flows with wide variation of Knudsen number. Truncated Wild (Wild 1951) sum expansion is employed to calculate time discretization, where the higher order collisions are replaced by the local Maxwellian distribution (Pareschi and Caflisch 1999). Pareschi and Russo (Pareschi and Russo

2000) performed the stability analysis on the TRMC method and proved the A-stability and L-stability of the method. They performed the TRMC method to study the Kac equation and obtained reasonable results compared to the results of the standard DSMC method. Moreover, Pareschi *et al.* (Pareschi and Wennberg 2001; Pareschi and Russo 2001a; Pareschi and Russo 2001b) introduced algorithm for the TRMC method using the variable hard sphere (VHS) molecules. They also studied the one-dimensional shock wave problem and obtained reasonable results compared to the results of DSMC method. Pareschi and Trazzi (Pareschi and Trazzi 2005) presented algorithms to obtain the first and second orders of the TRMC method that preserve the conservation of mass, momentum, and energy, simultaneously. They also studied the gas flow around an obstacle using the TRMC method and obtained an appreciable reduction in the CPU time, compared to the demanded CPU time for the standard DSMC method. Furthermore, Russo *et al.* (Russo, Pareschi, Trazzi, Shevyrin, Bondar, and Ivanov 2005) considered higher order collisions and introduced the third order of the TRMC method. They investigated the Couette flow for a variety of Knudsen numbers and several wall velocities using the TRMC and DSMC methods. Their study indicated that the density, velocity and temperature profiles, obtained from the TRMC method, are in excellent agreement with the ones from the DSMC method. Moreover, Ganjaei and Nourazar (Ganjaei and Nourazar 2009) studied binary Argon and Helium mixture flow inside a rotating cylinder using the DSMC and TRMC methods. They used Dalton's law for partial pressures of each species and showed that the results of TRMC method are in excellent agreement with the results obtained from analytical solution and standard DSMC method. Recently, Trazzi *et al.* (Trazzi, Pareschi, and Wennberg 2009) introduced recursive algorithm for the TRMC method to obtain uniform accuracy in time, independent from time step. They obtained considerable improvement in the computational efficiency of simulating the space homogeneous test cases and non-homogeneous stationary shock problem, in comparison to the standard DSMC method. Most recently, Eskandari and Nourazar (Eskandari and Nourazar 2017) performed the first, second and third orders of the TRMC scheme to study the lid-driven micro cavity flow with different lid velocities and Knudsen numbers. Furthermore, they employed the TRMC1, TRMC2 and TRMC3 schemes to investigate the flow over the nano plate with different free stream velocities and Knudsen numbers (Eskandari and Nourazar 2018). The investigations showed excellent agreement between the results obtained from the third order TRMC scheme with the ones from the standard DSMC method (Eskandari and Nourazar 2017; Eskandari and Nourazar 2018).

### 1.1 The Purpose of the Present Work

In the present work, it is intended to develop a modified method, called the MTRMC method, to reduce the computational CPU time of numerical solution of the Boltzmann equation compared to the

CPU time of the standard TRMC and DSMC methods.

To reach this aim, Taylor series expansion is employed in derivatives to reform the Wild sum expansion.

Simulation of a lid-driven micro cavity flow is considered as the benchmark problem to investigate the accuracy and computational expense of the proposed algorithm. The results obtained from the MTRMC method are compared with the results of the standard DSMC and TRMC methods. The present work intends to investigate the lid-driven micro cavity flow from the following points of view:

- Investigating the accuracy of proposed algorithm for the MTRMC method
- Comparison of demanded CPU time, demanded for the DSMC, TRMC and MTRMC methods studied cases
- Investigating the influence of lid velocity on the flow properties

## 2. MATHEMATICAL DESCRIPTION

### 2.1 Boltzmann Equation

The Boltzmann equation for a single component mono-atomic dilute gas in the absence of external forces, is described by the following form (Cercignani 1988; Bird 1994):

$$\frac{\partial f}{\partial t} + v \cdot \nabla_x = \frac{1}{Kn} Q(f, f). \quad (1)$$

The bilinear operator  $Q(f, f)$  describes the intermolecular binary collisions. Considering  $Q(f, f) = P(f, f) - \mu f$ , the Boltzmann equation takes the form below (Gabetta, Pareschi, and Toscani 1997; Wild 1951; Carlen, Carvalho, and Gabetta 2000):

$$\frac{\partial f}{\partial t} + v \cdot \nabla_x = \frac{1}{Kn} (P(f, f) - \mu f). \quad (2)$$

$P(f, f)$  is a symmetric bilinear operator describing the collision effect of the molecules and the parameter  $\mu = 0$  is the mean collision frequency. It is common to split the Boltzmann Eq. (2) into the equation of pure convection step (i.e.  $Q \equiv 0$ ) (3) and the equation of collision step (i.e.  $v \cdot \nabla_x \equiv 0$ )

(4) (Bird 1994; Pareschi and Trazzi 2005; Pareschi and Caflisch 1999; Trazzi, Pareschi, and Wennberg 2009; Jahangiri, Nejat, Samadi, and Aboutalebi 2012; Yanenko 1971).

$$\frac{\partial f}{\partial t} + v \cdot \nabla_x = 0. \quad (3)$$

$$\frac{\partial f}{\partial t} = \frac{1}{Kn} (P(f, f) - \mu f). \quad (4)$$

The equation of convection step can be directly solved leaving only concerns about the equation of collision step.

### 2.2 DSMC Approach

The DSMC approach can be obtained by applying the Euler upwind scheme to the equation of collision step (4):

$$\frac{f^{n+1} - f^n}{\Delta t} = \frac{\mu}{Kn} \frac{P(f, f)}{\mu} - \frac{\mu}{Kn} f. \quad (5)$$

$$f^{n+1} = \left(1 - \frac{\mu\Delta t}{Kn}\right) f^n + \frac{\mu\Delta t}{Kn} \frac{P(f, f)}{\mu}. \quad (6)$$

The DSMC scheme (6) can be probabilistically interpreted in the following way: In order to sample a particle from  $f^{n+1}$ , it shall be sampled from  $f^n$  with probability of  $1 - (\mu\Delta t/Kn)$  and shall be sampled from  $P(f, f)/\mu$  with probability of  $\mu\Delta t/Kn$ . Since the collision probability cannot accept negative values, then  $(\mu\Delta t/Kn) \leq 1$  (Pareschi and Trazzi 2005).

### 2.3 TRMC Approach

The relaxed time  $\tau$  and the transformed probability distribution function  $F(v, \tau)$  are described by the following form (Pareschi and Trazzi 2005; Pareschi and Caflisch 1999):

$$\tau = (1 - e^{-\mu/Kn}). \quad (7)$$

$$F(v, \tau) = f(v, \tau) e^{-\mu/Kn}. \quad (8)$$

Then by applying variables (7) and (8), Eq. (4) can be written as:

$$\begin{aligned} \frac{\partial F}{\partial \tau} &= \frac{1}{\mu} P(F, F). \\ F(v, \tau = 0) &= f(v, 0). \end{aligned} \quad (9)$$

The Cauchy problem (9) has a power series solution:

$$\begin{aligned} F(v, \tau) &= \sum_{k=0}^{\infty} \tau^k f_k(v). \\ f(v, t) &= e^{-\mu/Kn} \sum_{k=0}^{\infty} \left( (1 - e^{-\mu/Kn})^k f_k(v) \right). \end{aligned} \quad (10)$$

Rearranging Eq. (9) using Eq. (10) yields:

$$\frac{\partial F}{\partial \tau} = \sum_{k=0}^{\infty} k \tau^{k-1} f_k(v) = \sum_{k=0}^{\infty} (k+1) \tau^k f_{k+1}(v). \quad (11)$$

$$\begin{aligned} P(F, F) &= P\left(\sum_{k=0}^{\infty} \tau^k f_k(v), \sum_{k=0}^{\infty} \tau^k f_k(v)\right) \\ &= P(f_0, f_0) + 2\tau P(f_0, f_1) + \\ &+ \tau^2 (2P(f_0, f_2) + P(f_1, f_1)) + \dots \end{aligned} \quad (12)$$

Equating corresponding powers for the relaxation time, yields the recursive algorithm for the coefficients  $f_k$ :

$$f_{k+1} = \frac{1}{k+1} \sum_{h=0}^k \left( \frac{1}{\mu} P(f_k, f_{k-h}) \right). \quad (13)$$

Maxwellian truncation of Eq. (10) results in the TRMC scheme in the following way:

$$\begin{aligned} f^{n+1}(v) &= e^{-\mu\Delta t/Kn} \sum_{k=0}^m \tau^k f_k(v) \\ &+ \left(1 - e^{-\mu\Delta t/Kn}\right)^{m+1} M(v). \end{aligned} \quad (14)$$

It is noticeable that different weight functions may be used in the above formulations. Hence the general form of the TRMC method can be obtained by general form of weight functions (Pareschi and Caflisch 1999; Pareschi and Russo 2000; Pareschi and Russo 2001a; Pareschi and Russo 2001b; Pareschi and Trazzi 2005; Pareschi and Wennberg 2001; Trazzi, Pareschi, and Wennberg 2009):

$$f^{n+1}(v) = \sum_{k=0}^m (A_k f_k(v)) + A_{m+1} M(v). \quad (15)$$

where the coefficients  $f_k$  are determined by (13). In the present work, weight functions are selected in accordance with Pareschi (Pareschi and Trazzi 2005; Pareschi and Russo 2000).

$$\begin{aligned} A_k &= (1 - \tau) \tau^k \\ A_m &= 1 - \sum_{k=0}^m A_k - A_{m+1} \\ A_{m+1} &= \tau^{m+2}. \end{aligned} \quad (16)$$

The selected weight functions are non-negative functions that satisfy consistency (17), conservation (18) and asymptotic preservation (19), simultaneously.

$$\begin{aligned} \lim_{\tau \rightarrow 0} \frac{A_1(\tau)}{\tau} &= 1 \\ \lim_{\tau \rightarrow 0} \frac{A_k(\tau)}{\tau} &= 0, \quad \forall k = 0, \dots, m \end{aligned} \quad (17)$$

$$\sum_{k=0}^{m+1} A_k(\tau) = 1. \quad (18)$$

$$\begin{aligned} \lim_{\tau \rightarrow 1} A_k(\tau) &= 0, \quad \forall k = 0, \dots, m \\ \lim_{\tau \rightarrow 1} A_{m+1}(\tau) &= 1. \end{aligned} \quad (19)$$

It is noticeable that lower orders of the TRMC method may give inaccurate results for large time steps. On the other hand, computational complexity of the higher orders, is the main drawback of the TRMC method. Hence, in the present work, third order TRMC (TRMC3) method is used in all simulations.

Considering  $m = 3$  in the general form of the TRMC scheme (15) with the weight functions (16), yields the third order of the TRMC scheme:

$$\begin{aligned}
 f^{n+1} &= (1-\tau)f_0 + (\tau-\tau^2)\frac{P(f_0, f_0)}{\mu} \\
 &+ (\tau^2-\tau^3)\frac{P(f_0, f_1)}{\mu} \\
 &+ (\tau^3-\tau^5)\frac{2P(f_0, f_2)+P(f_1, f_1)}{3\mu} + \tau^5 M(v) \\
 &= A_0 f^n + A_1 f_1 + A_2 f_2 + A_3 f_3 + A_4 M(v).
 \end{aligned}
 \tag{20}$$

Eq. (20) can be probabilistically interpreted in the following way: A selected particle at the nth time step will be sampled from f1, f2 and local Maxwellian distribution with probabilities of, A1 and A2 respectively. The remaining particles existing in the f n distribution do not collide with probability of A0.

**2.4 MTRMC Approach**

In the MTRMC method, Taylor series expansion is employed to obtain derivatives with higher accuracies:

$$\frac{\partial F}{\partial \tau} = \frac{F^{n+1} - F^n}{\Delta \tau}. \tag{21}$$

$$F^{n+1} = \sum_{k=0}^m (\tau + \Delta \tau)^k f_k(v). \tag{22}$$

$$\Delta \tau = \frac{\partial \tau}{\partial t} \Delta t = \frac{\mu \Delta t}{Kn} e^{-\mu t / Kn}. \tag{23}$$

Introducing Eqs. (21) to (23), to Eq. (9) yields:

$$\frac{\sum_{k=0}^m (\tau + \Delta \tau)^k f_k - \sum_{k=0}^m \tau^k f_k}{\Delta \tau} = \frac{P(F, F)}{\mu} \tag{24}$$

Applying Eqs. (12) to Eq. (24) gives:

$$\begin{aligned}
 &\frac{((\tau + \Delta \tau)f_1 - \tau f_1) + ((\tau + \Delta \tau)^2 f_2 - \tau^2 f_2) + \dots}{\Delta \tau} \\
 &= \frac{1}{\mu} (P(f_0, f_0) + 2\tau P(f_0, f_1) + \dots).
 \end{aligned}
 \tag{25}$$

Coefficients fk can be obtained by rearranging the right and left hand sides of Eq. (25) for the same corresponding powers of the relaxation time:

$$\begin{aligned}
 f_1 &= \frac{\Delta \tau}{(\tau + \Delta \tau) - \tau} \frac{P(f_0, f_0)}{\mu} \\
 f_2 &= \frac{2\tau \Delta \tau}{(\tau + \Delta \tau)^2 - \tau^2} \frac{P(f_0, f_1)}{\mu} \\
 f_3 &= \frac{3\tau^2 \Delta \tau}{(\tau + \Delta \tau)^3 - \tau^3} \left( \frac{2P(f_0, f_2) + P(f_1, f_1)}{3\mu} \right)
 \end{aligned}
 \tag{26}$$

The MTRMC scheme can be obtained by applying a Maxwellian truncation to Eq. (10) with the coefficients fk in accordance with Eq. (26). Since the weight functions are non-unique, the general form of the MTRMC scheme can be illustrated in the following way:

$$f^{n+1} = \sum_{k=0}^m B_k f_k + B_{m+1} M(v). \tag{27}$$

Comparison of Eq. (27) with Eq. (6) indicates that for large Knudsen numbers (i.e. free molecular regimes) the MTRMC scheme behaves in the same way as the standard DSMC scheme, while the local Maxwellian distribution gradually replaces the time consuming collision terms as the Knudsen number decreases. Furthermore, for very small Knudsen numbers (i.e. at the fluid limit) the distribution function approaches the local Maxwellian distribution.

$$\begin{aligned}
 \lim_{\mu \Delta t / Kn \rightarrow 0} f^{n+1} &= f^n \\
 \lim_{\mu \Delta t / Kn \rightarrow \infty} f^{n+1} &= M(v).
 \end{aligned}
 \tag{28}$$

Considering the first three terms in the general form of the MTRMC scheme (27) with the weight functions (16), yields the third order of MTRMC scheme:

$$\begin{aligned}
 f^{n+1} &= f^n (1 - \tau \\
 &+ \frac{\tau^4 \Delta \tau (3\tau + 2\Delta \tau)(1 - \tau^2) + \tau^2 \Delta \tau (3\tau^2 + 3\tau \Delta \tau + \Delta \tau^2)(1 - \tau^3)}{(2\tau + \Delta \tau)(3\tau^2 + 3\tau \Delta \tau + \Delta \tau^2)}) \\
 &+ (\tau - \tau^2) \frac{P(f_0, f_0)}{\mu} \\
 &+ \left( \frac{(\tau^2 - \tau^3) \times 2\tau}{2\tau + \Delta \tau} \right) \frac{P(f_0, f_1)}{\mu} \\
 &+ \left( \frac{(\tau^3 - \tau^5) \times 3\tau^2}{3\tau^2 + 3\tau \Delta \tau + \Delta \tau^2} \right) \frac{2P(f_0, f_2) + P(f_1, f_1)}{3\mu} \\
 &+ \tau^5 M(v) \\
 &= B_0 f^n + B_1 \frac{P(f_0, f_0)}{\mu} + B_2 \frac{P(f_0, f_1)}{\mu} + B_3 M(v).
 \end{aligned}
 \tag{29}$$

The main advantage of the MTRMC method over the standard DSMC method is its ability in accepting larger time steps where, the time step is limited in the DSMC method ( $\mu \Delta t / Kn \leq 1$ ). It is noticeable that the mentioned limitation on the time step is resolved by defining relaxed time and transformed probability distribution function in the TRMC and MTRMC methods. On the other hand, comparison of Eqs. (20) and (29) indicates fewer collisions in the MTRMC method compared to the standard TRMC method. The fewer collisions can result in lower computational expense for the MTRMC method, compared to that of the standard TRMC method.

The third order of the MTRMC method can be formalized in the following algorithm:

**Algorithm 1** Third order MTRMC for VHS molecules

- 1: compute the initial velocity of the particles;
- 2: **for**  $t = 0$  to  $n_{tot} \Delta t$  **do**
- 3: mark all particles with the “0-collision” label

---

```

4: estimate upper bound for the cross-section
 $\bar{\sigma}$ ;
5: set  $\tau = (1 - e^{-\mu\Delta t/Kn})$ ;
6: compute  $B_1(\tau), B_2(\tau), B_3(\tau), B_4(\tau)$ ;
7: set  $N_1 = \lfloor NB_1/2 \rfloor, N_2 = \lfloor NB_2/4 \rfloor, N_3 = \lfloor NB_3/3 \rfloor, N_4 = \lfloor NB_4 \rfloor$ ;
8: select  $(N_1 + N_2 + N_3)$  dummy collision pairs among all particles;
9: for  $(N_1 + N_2 + N_3)$  pairs do
10: compute  $\sigma_{ij} = \sigma(|v_i - v_j|)$ ;
11: generate random number  $0 \leq \varepsilon \leq 1$ ;
12: if  $\varepsilon < (\sigma_{ij} / \bar{\sigma})$  then
13: perform the collision between particles  $i$  and  $j$ ;
14: compute the post collision velocities;
15: update the labels of participant particles to "1-collision";
16: end if
17: end for
18: select  $2N_2$  particles among "0-collision" and  $2N_2$  particles among "1-collision" particles;
19: for  $2N_2$  pairs do
20: perform the collision between pairs;
21: compute the post collision velocities;
22: update the labels of participant particles to "1-collision" and "2-collision";
23: end for
24: select  $N_3/3$  pairs among "1-collision" particles;
25: for pairs do
26: perform the collision between pairs;
27: compute the post collision velocities;
28: update the labels of participant particles to "2-collision";
29: end for
30: select  $N_3/3$  particles among "0-collision" and  $N_3/3$  particles among "2-collision" particles;
31: for  $N_3/3$  pairs do
32: perform the collision between pairs;
33: compute the post collision velocities;
34: update labels of participant particles to "1-collision" and "3-collision";
35: end for
36: for  $N_4$  particles do
37: replace particles with samples from the Maxwellian, with the same total energy and moment;
38: end for
39: for  $(N - 2N_1 - 4N_2 - 3N_3 - N_4)$  particles do
40: the energy and momentum will not change for remained particles;
41: end for
42: end for

```

---

### 3. GEOMETRY AND CALCULATION CONDITION

For validating the proposed modified time relaxed Monte Carlo (MTRMC) method, a lid-driven micro

cavity flow is considered. Figure 1 presents the configuration of the micro cavity geometry and the imposed boundary conditions. The cavity consists a square with a wall length of  $1\mu\text{m}$  where the walls are diffuse reflectors with surface temperatures of 300K. The walls are stationary except the upper lid which moves in the positive x direction. The cavity is initially filled with stationary mono-atomic Argon gas. Temperature, number density and Knudsen number of the Argon gas are 300K,  $2.59 \times 10^{26}$  molecules per cubic meter and 0.005, respectively. The Knudsen number is defined based on the wall length. Moreover, three different velocities are considered for the moving lid. The lid velocities are 10m/s, 100m/s and 1000m/s for cases I, II and III, respectively. Selected velocities are typical lid velocities to investigate the micro cavity flow in low Knudsen number regimes (Amiri-Jaghargh, Roohi, Niazmand, and Stefanov 2012; Amiri-Jaghargh, Roohi, Niazmand, and Stefanov 2013; Mohammadzadeh, Roohi, and Niazmand 2013; John, Gu, and Emerson 2011; John, Gu, and Emerson 2010; Jiang, Fan, and Shen 2003; Sheremet and Pop 2015; Safdari and Kim 2015; Gutt and Groan 2015; Rana, Torrilhon, and Struchtrup 2013).

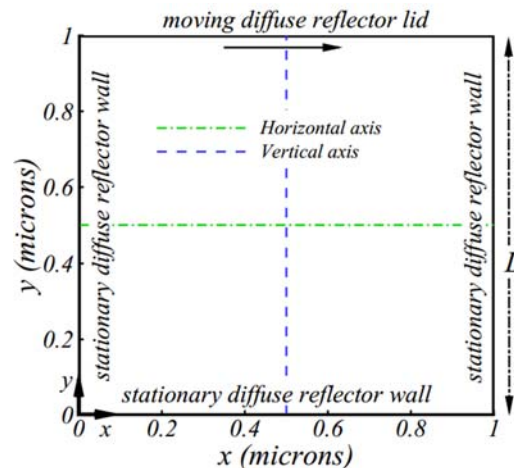


**Fig. 1. Lid-driven micro cavity geometry and the imposed boundary conditions.**

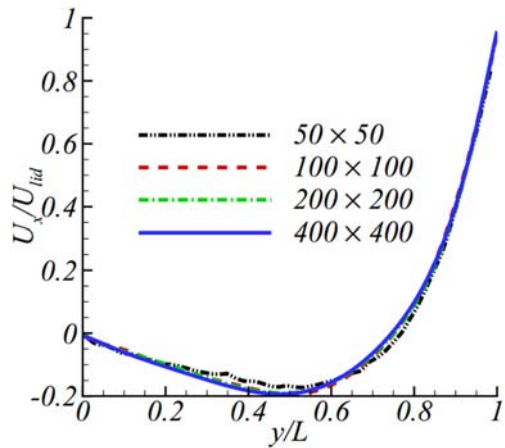
Variable hard sphere (VHS) scheme is considered for the molecular collisions. The reference molecular diameter, viscosity index and molecular mass are set to  $4.17 \times 10^{-17}\text{m}$ , 0.81 and  $66.3 \times 10^{-27}\text{kg}$ , respectively (Bird 1994).

In the present study, the time step in the DSMC method is computed considering the limitation  $\mu\Delta t/Kn \leq 0$  (see Eq. (6)) while for the TRMC and MTRMC methods, the time step is chosen to be a fraction of the free flow time step,  $C\Delta t$ , where  $C \leq 1$  is a constant. The parameter C is set to 0.4, 0.35 and 0.18 for cases I, II and III, respectively.

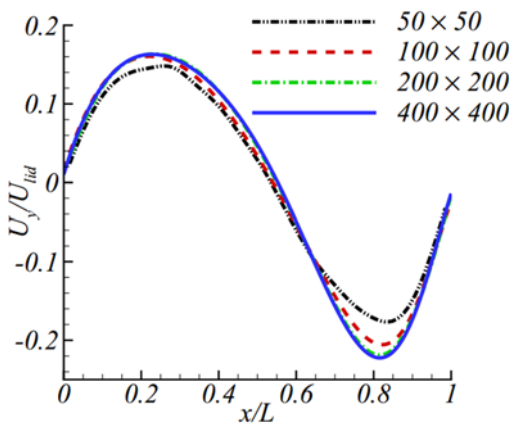
#### 3.1 Grid independency test

The finer cell size yields more accurate results but increases computational expenses. A grid independency study is carried out using the four grid resolutions of  $50 \times 50$ ,  $100 \times 100$ ,  $200 \times 200$  and 400

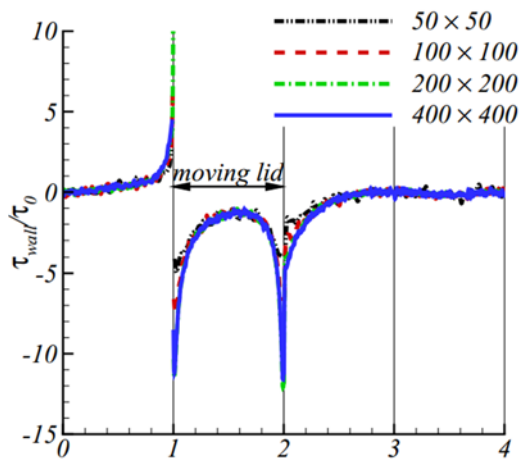
× 400 cells (Amiri-Jaghargh, Roohi, Niazmand, and Stefanov 2012; Amiri-Jaghargh, Roohi, Niazmand, and Stefanov 2013; Amiri-Jaghargh, Roohi, Stefanov, Nami, and Niazmand 2014; Stefanov 2011; Roohi and Stefanov 2016). All cells are uniform in x and y directions and consist of four sub-cells.



(a)  $U_x$  distribution along the vertical axis.



(a)  $U_y$  distribution along the horizontal axis.



(b) Wall shear stress distribution.

**Fig. 2. Grid independency tests.**

To ensure reaching independent grids, the

distributions of the x-component and y-component of velocity vector ( $U_x$  and  $U_y$ , respectively) along the vertical and horizontal axes in addition to the wall shear stress distributions are investigated. Figure 2(a) indicates that  $U_x$  is not significantly affected by fine grids while Fig. 2(b) presents enormous error for  $U_y$  in coarse grids. This may be attributed to the higher velocity gradients along the cavity horizontal axis rather than the vertical axis. Moreover, Fig. 2(c) illustrates that simulation errors for coarse grains are more pronounced on the moving lid. This may also be attributed to the higher gradients on the moving lid compared to that on stationary walls. A grid resolution of  $400 \times 400$  is used in the present study to obtain the results in-dependent of grid resolution. Furthermore, since 3,300,000 particles on the average are considered, it is expected to have 20 particles per cell on the average.

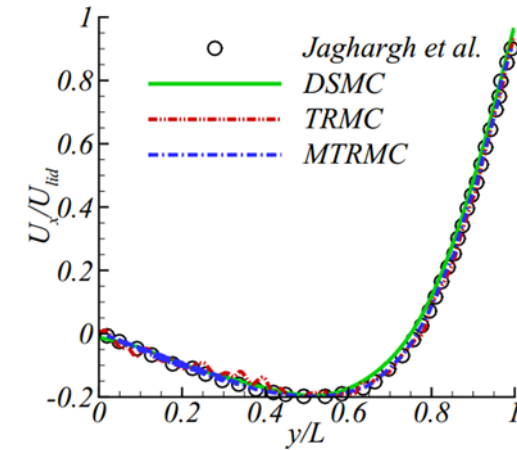
#### 4. INVESTIGATING THE RESULTS OBTAINED FROM THE MTRMC METHOD

In this section the results obtained from the MTRMC method are presented. For validation purpose, a detailed comparison between the results obtained from the MTRMC method with those from the standard TRMC method (carried out in the present study) and the results from the standard DSMC method with either NTC or SBT collision sampling schemes (Amiri-Jaghargh, Roohi, Niazmand, and Stefanov 2012; Amiri-Jaghargh, Roohi, Niazmand, and Stefanov 2013; Amiri-Jaghargh, Roohi, Stefanov, Nami, and Niazmand 2014; Stefanov 2011; Roohi and Stefanov 2016), are made.

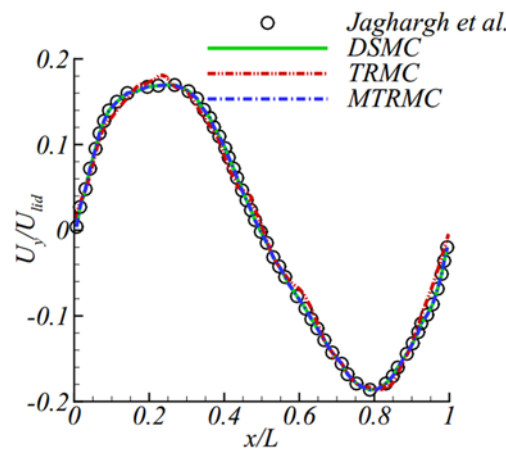
Figure 3 illustrates the non-dimension wall shear stress distributions and the distributions of x and y components of velocity vector along the cavity axes in the lid-driven micro cavity flow for case I ( $U_{lid} = 10\text{m/s}$ ). The reference shear stress is defined as  $\tau_0 = \mu_0 \times U_{lid}/L$ . The results obtained from the MTRMC method are compared with those from the standard TRMC method and the standard DSMC method with either NTC or SBT collision sampling schemes (Amiri-Jaghargh, Roohi, Niazmand, and Stefanov 2012; Amiri-Jaghargh, Roohi, Niazmand, and Stefanov 2013; Amiri-Jaghargh, Roohi, Stefanov, Nami, and Niazmand 2014; Stefanov 2011; Roohi and Stefanov 2016) for case I. Figure 3 illustrates excellent agreement between the results of the MTRMC method and those from the standard TRMC and DSMC methods (Amiri-Jaghargh, Roohi, Niazmand, and Stefanov 2013).

Figure 4 presents the distributions of non-dimension velocity and wall shear stress of the cavity flow for case II ( $U_{lid} = 100\text{m/s}$ ). The distributions illustrate excellent agreement between the results of MTRMC method with those from the TRMC method the standard DSMC method with either NTC or SBT collision sampling schemes (Amiri-Jaghargh, Roohi,

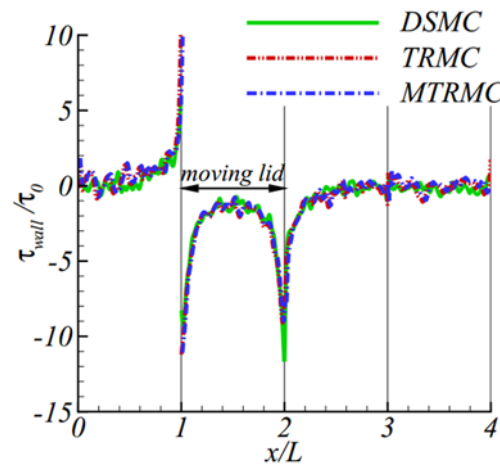
Niazmand, and Stefanov 2012; Amiri-Jaghargh, Roohi, Niazmand, and Stefanov 2013). Moreover, Fig. 4(c) indicates that the maximum wall shear stress occurs at both ends of the moving lid. This may be attributed to higher velocity gradients at both ends of the moving lid.



(a)  $U_x$  distribution along the vertical axis.

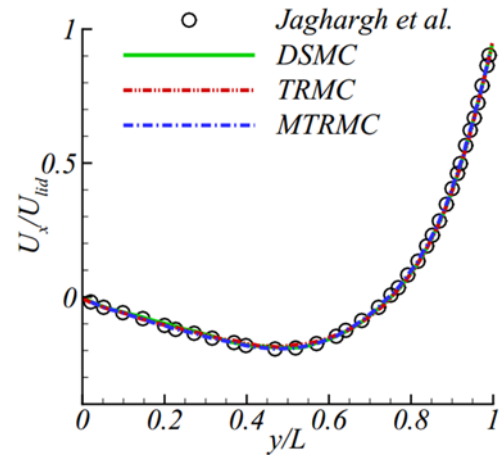


(a)  $U_y$  distribution along the horizontal axis.

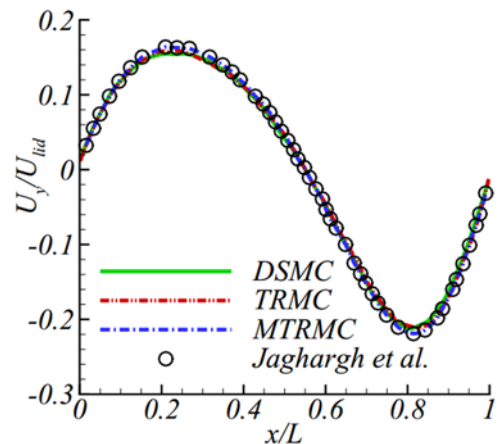


(b) Wall shear stress distribution.

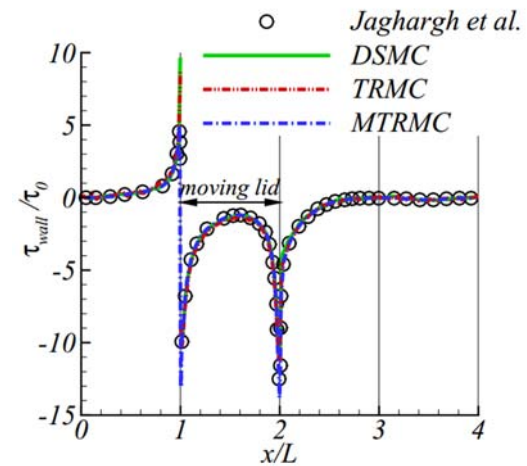
**Fig. 3. Velocity and shear stress distributions for case I ( $U_{lid} = 10\text{m/s}$ ).**



(a)  $U_x$  distribution along the vertical axis.



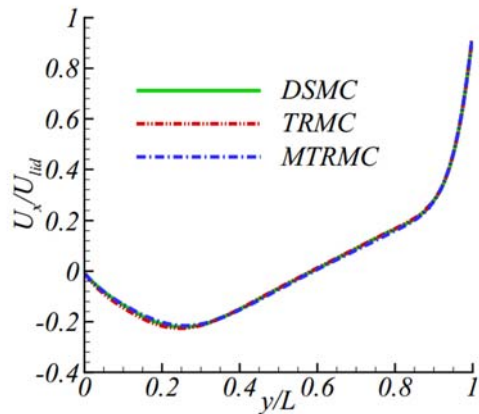
(a)  $U_y$  distribution along the horizontal axis.



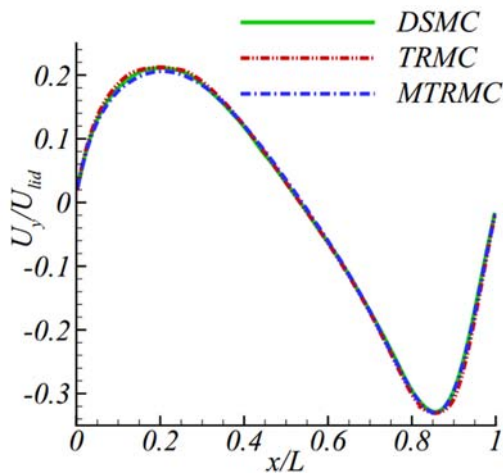
(b) Wall shear stress distribution.

**Fig. 4. Velocity and wall shear stress distributions for case II ( $U_{lid} = 100\text{m/s}$ ).**

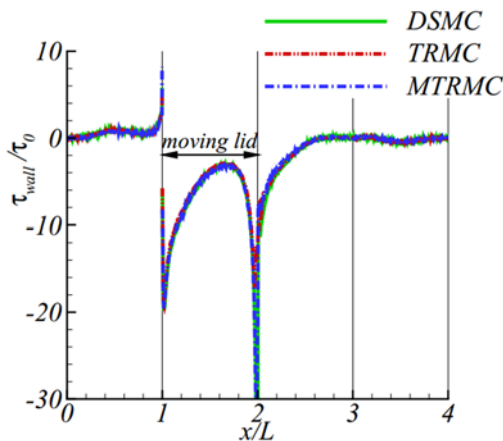
Figure 5 presents the distributions of  $U_x/U_{lid}$ ,  $U_y/U_{lid}$  and  $\tau_{wall}/\tau_0$  along the vertical axes, horizontal axes and cavity walls, respectively for case III ( $U_{lid} = 1000\text{m/s}$ ). The comparisons show excellent agreement between results of the MTRMC method and those obtained from the TRMC and DSMC methods.



(a)  $U_x$  distribution along the cavity axes.



(b)  $U_y$  distribution along the horizontal axis.



(c) Wall shear stress distribution.

**Fig. 5. Velocity and wall shear stress distributions for case II ( $U_{lid} = 1000\text{m/s}$ ).**

Figures 3 to 5 demonstrate that the results of MTRMC method show excellent agreement with their counterparts from the standard TRMC and DSMC method for a wide range of lid velocities including low subsonic (i.e.  $U_{lid} = 10\text{m/s}$ ) to supersonic (i.e.  $U_{lid} = 1000\text{m/s}$ ) lid velocities.

Figure 6 presents the CPU time against the physical time at different lid velocities for the DSMC, TRMC and MTRMC methods. Figure 6 indicates

that for the same physical time, the demanded CPU time for the DSMC and TRMC methods is greater than that for the MTRMC method. The enormous difference between the computational costs of the MTRMC and DSMC methods originates from replacing the time consuming intermolecular collision with the local Maxwellian distribution (see Eqs. (6) and (29)) and using the relaxed time which allows employing higher time steps, while the improvement in comparison to the TRMC method, can be attributed to the modified collision functions which yield fewer intermolecular collisions in the MTRMC method compared to the standard TRMC method (see Eqs. (20) and (29)).

**Table 1 Normalized CPU time for the DSMC, TRMC and MTRMC schemes at different lid velocities**

	10	100	500	800	1000
DSMC	1.000	1.000	1.000	1.000	1.000
TRMC	0.958	0.934	0.561	0.512	0.484
MTRMC	0.912	0.881	0.512	0.463	0.439

Table 1 presents the normalized consumed CPU time for DSMC, TRMC and MTRMC methods in the present work, at different lid velocities. The comparison of the consumed CPU times indicate that for the same physical time, the CPU time required for the MTRMC method to simulate the lid-driven micro cavity flow accurately, is comparably less than those of the DSMC and TRMC methods. The improvement in the demanded CPU time of MTRMC method compared to the DSMC method, is more pronounced as the lid velocities increase.

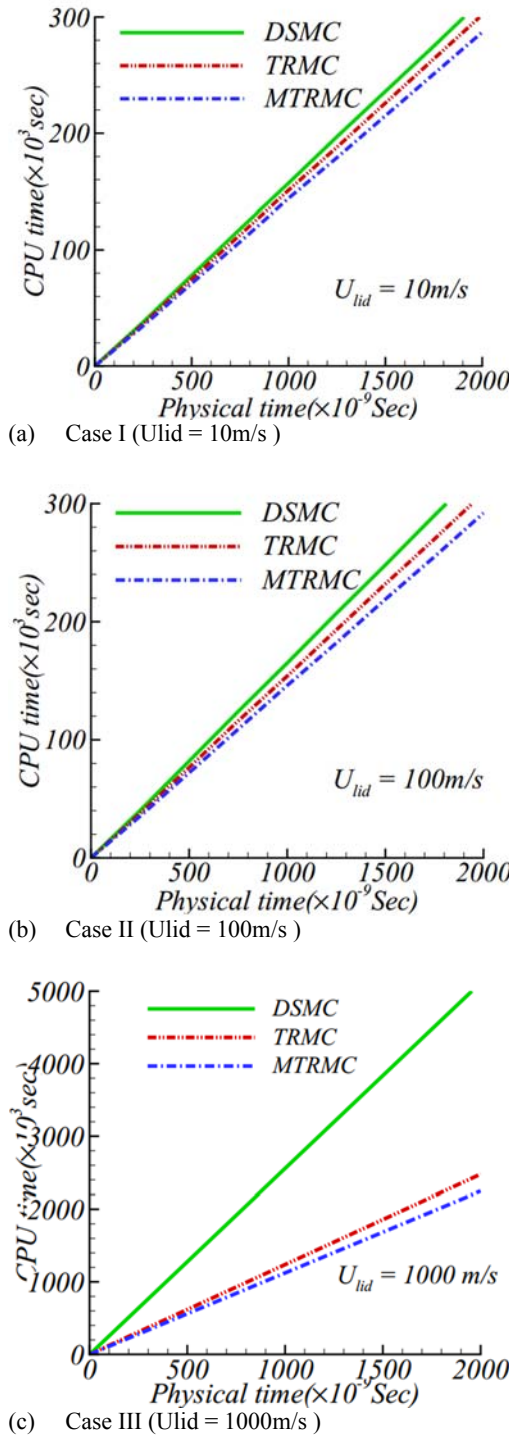
Figure 7 presents the reduction in the demanded CPU time for the MTRMC method in comparison to the ones from the standard DSMC method. Figure 7 indicates that as the lid velocity increases, the reduction in the demanded CPU time for the MTRMC method to simulate the micro cavity flow accurately, significantly increases. This is more pronounced for higher lid velocities where, for values of lid velocities higher than  $1000\text{m/s}$  the reduction in the CPU time approaches an asymptotic value of about 58%.

Figure 7 and table 1 showed that the difference between the MTRMC and the DSMC schemes about the computational costs becomes significant for the lid velocities  $U_{lid} \geq 500\text{(m/s)}$ .

## 5. COMPARISON OF THE RESULTS FOR DIFFERENT LID VELOCITIES

In this section, the validated results obtained from the MTRMC method for different lid velocities, are compared. It should be indicated that the Knudsen number, based on the wall length is considered to be  $Kn = 0.005$  (see section 3.). Figure 8 presents the normalized  $U_x, U_y$  and  $\tau_{wall}$  distributions in the micro cavity flow with different lid velocities, varying from low to very high supersonic velocities. It indicates that for lid velocities up to  $100\text{m/s}$ , including cases I and II, the velocity distribution patterns are almost the same. However, for higher lid

velocities, including case III with  $U_{lid} = 1000\text{m/s}$ , different velocity distribution patterns with higher near wall velocity gradients are observed. Moreover, shear stress distributions illustrate the same pattern for lid velocities below  $100\text{m/s}$  while for case III with  $U_{lid} = 1000\text{m/s}$ , higher shear stresses are observed. The higher stress may be attributed to higher near wall velocity gradients.



**Fig. 6. Comparison of physical time and CPU time of different schemes and different lid velocities.**

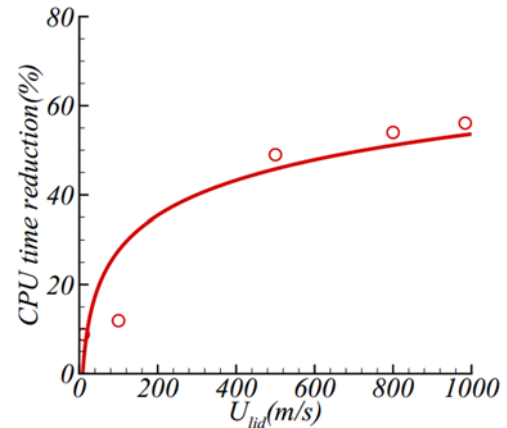


**Fig. 7. Reduction of CPU time in the MTRMC method compared to the standard DSMC method.**

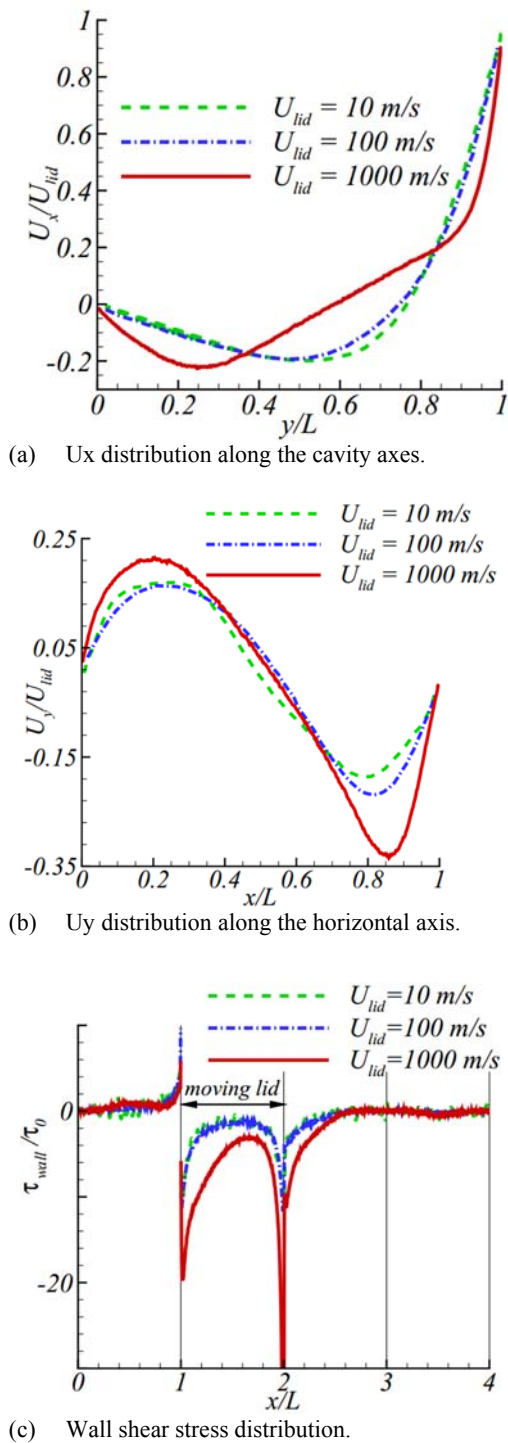
Figure 9 presents the velocity streamlines superimposed on the temperature contours for different lid velocities obtained from the MTRMC method. It is observed that the maximum temperature in the cavity flow increases significantly as the lid velocity increases. The increase in the temperature for case I is negligible while the temperature rise for case III is substantial and the flow field consists of a hot spot near the moving lid. The hot spot may be attributed to the formation of the shock wave in case III. Moreover, It is found that the formation of secondary vortices is enhanced as the lid velocity increases. Furthermore the streamlines lose their symmetry as the lid velocity increases.

Table 2 presents primary vortex center location for different lid velocities, obtained from the MTRMC scheme. The comparison of the results with their counterparts reported by Jaghargh *et al.* (Amiri-Jaghargh, Roohi, Niazmand, and Stefanov 2013) indicates that the MTRMC scheme can simulate the velocity streamlines accurately.

**Table 2. Primary vortex center location for different lid velocities.**

Re	$U_{lid}$ (m/s)	Primary vortex center location ( $x_c/L; y_c/L$ ) (present work)	Primary vortex center location ( $x_c/L; y_c/L$ ) (Jaghargh <i>et al.</i> )
9.16	10	(0.51,0.76)	(0.51,0.76)
91.58	100	(0.61,0.75)	(0.61,0.75)
915.79	1000	(0.55,0.59)	-

Figure 10 presents contour of the local Mach number for case III ( $U_{lid} = 1000\text{m/s}$ ) and  $Kn = 0.005$  with the iso-values of Mach = 1 determined in bold black lines. The illustrated shock wave results in significantly high amount of shear stress and energy dissipation. It is observed that.

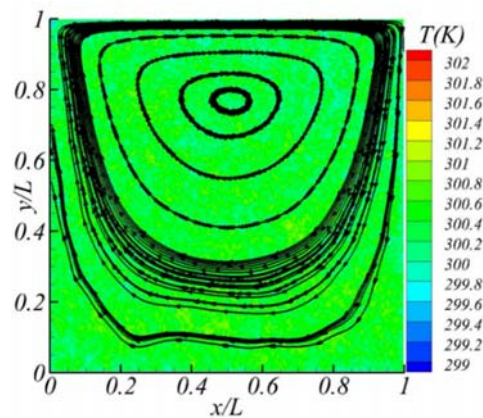


**Fig. 8. Velocity and shear stress distributions for different lid velocities and  $Kn = 0.005$ .**

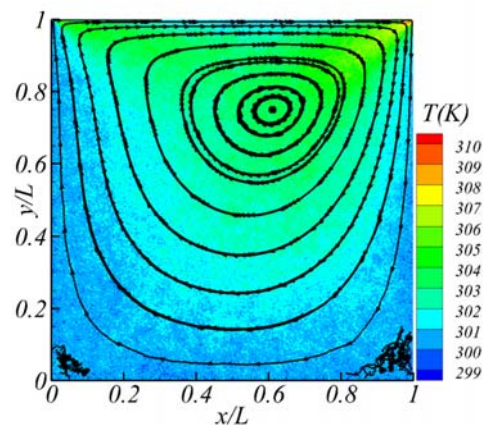
## 6. CONCLUSION

In the present work, the modified time relaxed Monte Carlo (MTRMC) method has been introduced. Taylor series expansion is employed in the Wild sum expansion to obtain the modified collision functions with fewer intermolecular collision. It is observed that the proposed algorithm for the MTRMC method is capable to accurately simulate the lid-driven micro cavity flow with different lid velocities, covering low subsonic to supersonic lid velocities. Moreover, it is

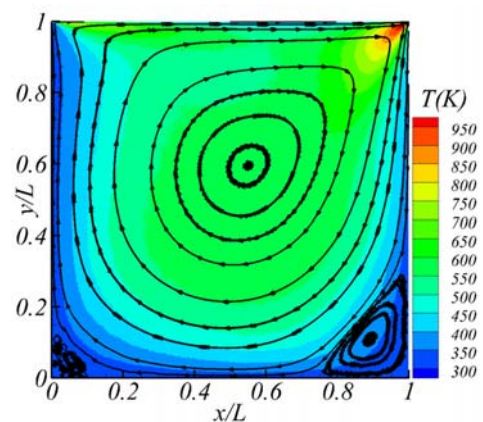
illustrated that for the same physical time, the computational CPU time of the MTRMC method is appreciably less than that for the standard DSMC and TRMC methods. The reduction in the computational CPU time is enhanced at higher lid velocities. The improvement in the CPU time is more pronounced when the comparison is made with the standard DSMC method with either NTC or SBT collision sampling scheme. It is shown that up to 56% reduction in the computational CPU time can be obtained from MTRMC method compared to the standard DSMC method.



(a) Case I ( $U_{lid} = 10$  m/s)



(b) Case II ( $U_{lid} = 100$  m/s)



(c) Case III ( $U_{lid} = 1000$  m/s)

**Fig. 9. Velocity streamlines superimposed on the temperature contours for different lid velocities and  $Kn = 0.005$ .**

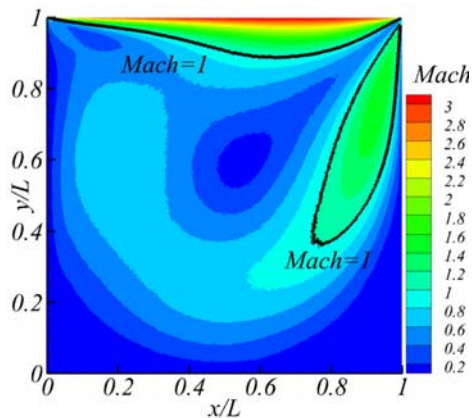


**Fig. 10. Contours of local Mach number for case III (Ulid = 1000m/s) and Kn = 0.005.**

### REFERENCES

- Amiri Jaghargh, A., E. Roohi, H. Niazmand and S. Stefanov (2012). Low speed/low rarefaction flow simulation in micro/nano cavity using DSMC method with small number of particles per cell. *Journal of Physics: Conference Series* 362, 012007.
- Amiri-Jaghargh, A., E. Roohi, H. Niazmand and S. Stefanov (2013). DSMC Simulation of Low Knudsen Micro/Nanoflows Using Small Number of Particles per Cells. *Journal of Heat Transfer* 135(10), 101008.
- Amiri-Jaghargh, A., E. Roohi, S. Stefanov, H. Nami and H. Niazmand (2014). DSMC simulation of micro/nano flows using SBTTAS technique. *Computers & Fluids* 102, 266–276.
- Bird, G. A. (1994). *Molecular Gas Dynamics and the Direct Simulation of Gas Flows*. Oxford: Clarendon Press.
- Carlen, E. A., M. C. Carvalho and E. Gabetta (2000). Central limit theorem for Maxwellian molecules and truncation of the wild expansion. *Communications on Pure and Applied Mathematics* 53(3), 370–397.
- Cercignani, C. (1988). *The Boltzmann Equation and Its Applications*, Volume 67 of Applied Mathematical Sciences. New York, NY: Springer New York.
- Eskandari, M. and S. Nourazar (2017). On the time relaxed Monte Carlo computations for the lid-driven micro cavity flow. *Journal of Computational Physics* 343, 355–367.
- Eskandari, M. and S. Nourazar (2018). On the time relaxed Monte Carlo computations for the flow over a flat nanoplate. *Computers & Fluids* 160, 219–229.
- Filbet, F. and G. Russo (2003). High order numerical methods for the space non-homogeneous Boltzmann equation. *Journal of Computational Physics* 186(2), 457–480.
- Gabetta, E., L. Pareschi and G. Toscani (1997). Relaxation Schemes for Nonlinear Kinetic Equations. *SIAM Journal on Numerical Analysis* 34(6), 2168–2194.
- Ganjaei, A. A. and S. S. Nourazar (2009). Numerical simulation of a binary gas flow inside a rotating cylinder. *Journal of Mechanical Science and Technology* 23(10), 2848–2860.
- Gutt, R. and T. Groan (2015). On the lid-driven problem in a porous cavity. A theoretical and numerical approach. *Applied Mathematics and Computation* 266, 1070–1082.
- Jahangiri, P., A. Nejat, J. Samadi and A. Aboutalebi (2012). A high-order Monte Carlo algorithm for the direct simulation of Boltzmann equation. *Journal of Computational Physics* 231(14), 4578–4596.
- Jiang, J.-Z., J. Fan and C. Shen (2003). *Statistical Simulation of Micro-Cavity Flows*. In AIP Conference Proceedings, Volume 663, pp. 784–791. AIP.
- John, B., X.-J. Gu and D. Emerson (2010). Investigation of Heat and Mass Transfer in a Lid-Driven Cavity Under Nonequilibrium Flow Conditions. *Numerical Heat Transfer, Part B: Fundamentals* 58(5), 287–303.
- John, B., X.-J. Gu and D. R. Emerson (2011). Effects of incomplete surface accommodation on non-equilibrium heat transfer in cavity flow: A parallel DSMC study. *Computers & Fluids* 45(1), 197–201.
- Mohammadzadeh, A., E. Roohi and H. Niazmand (2013). A Parallel DSMC Investigation of Monatomic/Diatomic Gas Flows in a Micro/Nano Cavity. *Numerical Heat Transfer, Part A: Applications* 63(4), 305–325.
- Oran, E. S., Oh, C. K. and B. Z. Cybyk (1998). DIRECT SIMULATION MONTE CARLO: Recent Advances and Applications. *Annual Review of Fluid Mechanics* 30(1), 403–441.
- Pan, L. S., G. R. Liu, B. C. Khoo and B. Song (2000). A modified direct simulation Monte Carlo method for low-speed microflows. *Journal of Micromechanics and Microengineering* 10(1), 21–27.
- Pareschi, L. and B. Wennberg (2001). A recursive Monte Carlo method for the Boltzmann equation in the Maxwellian case. *Monte Carlo Methods and Applications* 7(3-4).
- Pareschi, L. and G. Russo (2000). Asymptotic preserving Monte Carlo methods for the Boltzmann equation. *Transport Theory and Statistical Physics* 29(3-5), 415–430.
- Pareschi, L. and G. Russo (2001a). *An introduction to Monte Carlo method for the Boltzmann equation*. ESAIM: Proceedings 10, 35–75.
- Pareschi, L. and G. Russo (2001b). Time Relaxed Monte Carlo Methods for the Boltzmann Equation. *SIAM Journal on Scientific Computing* 23(4), 1253–1273.

- Pareschi, L. and R. E. Caflisch (1999). An Implicit Monte Carlo Method for Rarefied Gas Dynamics. *Journal of Computational Physics* 154(1), 90–116.
- Pareschi, L. and S. Trazzi (2005). Numerical solution of the Boltzmann equation by time relaxed Monte Carlo (TRMC) methods. *International Journal for Numerical Methods in Fluids* 48(9), 947–983.
- Rana, A., M. Torrilhon and H. Struchtrup (2013). A robust numerical method for the R13 equations of rarefied gas dynamics: Application to lid driven cavity. *Journal of Computational Physics* 236, 169–186.
- Roohi, E. and S. Stefanov (2016). Collision partner selection schemes in DSMC: From micro/nano flows to hypersonic flows. *Physics Reports* 656, 1–38.
- Russo, G., L. Pareschi, S. Trazzi, A. A. Shevyrin, Y. A. Bondar and M. S. Ivanov (2005). *Plane Couette Flow Computations by TRMC and MFS Methods*. In AIP Conference Proceedings, Volume 762, 577–582. AIP.
- Safdari, A. and K. C. Kim (2015). Lattice Boltzmann simulation of the three-dimensional motions of particles with various density ratios in lid-driven cavity flow. *Applied Mathematics and Computation* 265, 826–843.
- Sheremet, M. and I. Pop (2015). Mixed con-vection in a lid-driven square cavity filled by a nanofluid: Buongiorno’s mathematical model. *Applied Mathematics and Computation* 266, 792–808.
- Stefanov, S. K. (2011). On DSMC Calculations of Rarefied Gas Flows with Small Number of Particles in Cells. *SIAM Journal on Scientific Computing* 33(2), 677–702.
- Trazzi, S., L. Pareschi and B. Wennberg (2009). Adaptive and Recursive Time Relaxed Monte Carlo Methods for Rarefied Gas Dynamics. *SIAM Journal on Scientific Computing* 31(2), 1379–1398.
- Wild, E. (1951). *On Boltzmann’s equation in the kinetic theory of gases*. Mathematical Proceedings of the Cambridge Philosophical Society 47(03), 602.
- Yanenko, N. N. (1971). *The Method of Fractional Steps*. Berlin, Heidelberg: Springer Berlin Heidelberg.